Silanes and germanes as free-radical reducing agents: an *ab initio* study of hydrogen atom transfer from some trialkylsilanes and germanes to alkyl radicals

Dainis Dakternieks,[a] David J. Henry[a] and Carl H. Schiesser *[,b]

[a] *School of Biological and Chemical Sciences, Deakin University, Geelong, Victoria, Australia, 3217*
[b] *School of Chemistry, The University of Melbourne, Parkville, Victoria, Australia, 3052*

Ab initio **molecular orbital calculations using a (valence) double-ζ pseudopotential (DZP) basis set, with (MP2, QCISD) and without (SCF) the inclusion of electron correlation predict that hydrogen atoms, methyl, ethyl, isopropyl and *tert*-butyl radicals abstract hydrogen atom from silane, methylsilane, dimethylsilane, trimethylsilane, trisilylsilane and the analogous germanes *via* transition states in which the attacking and leaving radicals adopt colinear (or nearly so) arrangements. Except for reactions involving trisilylsilane which are predicted at the MP2/DZP level to involve transition states with Si–C distances of about 3.19 Å, transition states which have (overall) Si–C and Ge–C separations of 3.12–3.15 and 3.24–3.26 Å respectively are calculated; these distances appear to be independent of the number of methyl substituents on the group(IV) element, but appear to be slightly sensitive to the nature of the attacking radical, with marginally earlier transition states calculated as the degree of alkyl substitution on the attacking radical is increased. At the highest level of theory (QCISD/DZP//MP2/DZP), energy barriers ($\Delta E_1^{\ddagger}$) of 27–57 (Si) or 26–44 (Ge) kJ mol^{-1} are predicted for the forward reactions, while the reverse reactions ($\Delta E_2^{\ddagger}$) are calculated to require 85–134 (Si) or 102–138 (Ge) kJ mol^{-1}. These values are marginally affected by the inclusion of zero-point vibrational energy correction. Importantly, QCISD and MP2 calculations appear to predict correctly the relative ordering of activation energies for alkyl radical reduction by silanes: tertiary < secondary < primary; SCF/DZP, AM1 and AM1 (CI = 2) calculations perform somewhat more poorly in their prediction of relative radical reactivity.**

Introduction

Silanes, germanes and stannanes play important roles as chain-carriers in free-radical chemistry;[1–4] a typical chain reaction is illustrated in reactions (1)–(3). While reagents such as tributyltin hydride and triphenyltin hydride have dominated synthetic procedures involving radical chemistry over the past two decades,[1] problems associated with product purification[4,5] and, more recently, toxicity[6] have necessitated the development of more user and environmentally friendly reagents. Despite the inherent expense involved in the use of germanium-based reagents, there are several reports detailing the use of trialkylgermanes in radical chemistry.[1,7] Tributylgermane, for example, can often be utilised in circumstances where a slower delivery of hydrogen is required, thereby resulting in increased yields of products arising during radical rearrangement strategies.

$$R_3SiH + init \longrightarrow R_3Si^{\bullet} \quad (1)$$

$$R'X + R_3Si^{\bullet} \longrightarrow R'^{\bullet} + R_3SiX \quad (2)$$

$$R'^{\bullet} + R_3SiH \longrightarrow R'H + R_3Si^{\bullet} \quad (3)$$

In addition, trialkylsilanes offer the synthetic chemist several advantages over the more traditional tin-based reagents; these include superior chromatographic properties, low toxicity and better inherent stability.[6,8] Despite these advantages, trialkylsilanes suffer from one major drawback; the Si–H bond strength in most trialkysilanes (*ca.* 460 kJ mol^{-1}),[9] with associated rate constants (k_H) of about 600 M^{-1} s^{-1} for the transfer of hydrogen atom to primary alkyl radicals,[9] leads to poor radical chain propagation. The inability to sustain chain reactions involving the delivery of a hydrogen atom as a key chain-propagating step renders most readily available silanes inappropriate for radical based syntheses.[2]

Triphenylsilane, with a rate constant (k_H) of some 5×10^4 M^{-1} s^{-1} (110 °C) for the delivery of hydrogen atom to primary alkyl radicals sits at the border of acceptable reactivity and can often be used in radical chain reactions.[1,9] More recently tris(trimethylsilyl)silane (TTMSS) has been developed to overcome several of the disadvantages of both silane and stannane based reagents.[6] With a rate constant (k_H) of 4×10^5 M^{-1} s^{-1} (27 °C) for the delivery of hydrogen atom to primary alkyl radicals, TTMSS behaves much more like tributyltin hydride [$k_H = 2 \times 10^6$ M^{-1} s^{-1} (25 °C)] in its radical chain-propagating properties.[10] This, together with superior chromatographic properties and low toxicity, has led to this relative newcomer in radical chemistry being widely accepted as the reagent of choice in many free-radical reactions.[2,9]

As part of our continuing interest in the development of new reagents for use in free-radical chemistry, we modelled the radical reactions of several silanes and germanes with alkyl radicals through the use of *ab initio* molecular orbital theory using a (valence) double-ζ pseudopotential (DZP) basis set with (MP2, QCISD) and without (SCF) the inclusion of electron correlation. We established previously that the DZP basis set behaves more like a triple-ζ all-electron basis for many higher heteroatoms;[11] specific to this work are DZP results obtained for homolytic substitution reactions involving silicon which were found to be very similar to those obtained using 6-311G**, both with and without the inclusion of electron correlation.[12] While DZP offers only minor cost advantages over 6-311G** for silicon, we nevertheless chose this basis set for consistency with our other studies[14] where significant cost advantages were enjoyed. Our recently published computational study of hydrogen abstractions from stannane and trimethylstannane provided valuable geometric

Table 1 Calculated energy barriers[a] for the forward ($\Delta E_1^{\ddagger}$) and reverse ($\Delta E_2^{\ddagger}$) hydrogen atom abstraction reactions of hydrogen atom with silane (SiH_4), methylsilane ($MeSiH_3$), dimethylsilane (Me_2SiH_2), trimethylsilane (Me_3SiH) and trisilylsilane [$(H_3Si)_3SiH$] (Scheme 1, R = H, Y = R′$_3$Si) and transition state (imaginary) frequency (ν)[b] of structures **1**–**5**

Y	TS	Method	$\Delta E_1^{\ddagger}$	$\Delta E_1^{\ddagger}$ + ZPVE[c]	$\Delta E_2^{\ddagger}$	$\Delta E_1^{\ddagger}$ + ZPVE[c]	ν
H_3Si	**1**	SCF/DZP	80.2	78.0	102.0	98.0	2110i
		MP2/DZP	48.4	45.4	96.5	92.9	1887i
		QCISD/DZP[d]	35.5	[32.5]	97.7	[94.1]	—
MeH_2Si	**2**	SCF/DZP	68.5	64.5	99.1	94.0	2071i
		MP2/DZP	47.8	(43.8)	92.7	87.6	—
		QCISD/DZP[d]	38.5	(34.5)	94.0	88.9	—
Me_2HSi	**3**	SCF/DZP	69.0	65.1	95.9	90.1	2027i
		MP2/DZP	47.1	(43.2)	88.4	(82.6)	—
		QCISD/DZP[d]	38.0	(34.1)	89.9	(84.1)	—
Me_3Si	**4**	SCF/DZP	69.4	65.6	93.2	86.0	1980i
		MP2/DZP	46.2	(42.4)	84.2	(77.0)	—
		QCISD/DZP[d]	37.3	(33.5)	85.9	(78.7)	—
$(H_3Si)_3Si$	**5**	SCF/DZP	54.3	51.2	118.4	110.6	2040i
		MP2/DZP	33.9	(30.8)	111.1	(103.3)	—
		QCISD/DZP[d]	26.8	(23.7)	116.6	(108.8)	—

[a] Energies in kJ mol^{-1}. [b] Frequencies in cm^{-1}. [c] Values in parentheses are estimates based on SCF/DZP ZPE corrections. Values in square brackets are estimated based on MP2/DZP ZPE corrections. [d] QCISD/DZP//MP2/DZP.

details of the transition states involved in the delivery of hydrogen atom to alkyl radicals, details which could not be obtained by experimental methods.[14] In a similar manner, studies involving silicon and germanium are expected to provide insight into reactions involving silane and germane based reagents and aid in the development of modified silanes and germanes.

To the best of our knowledge there are few *ab initio* studies involving silyl[8,9,15–19] and germyl radicals.[11] In order to provide further insight into the details of hydrogen atom transfer from silanes and germanes, we have examined the potential energy surfaces for the attack of hydrogen atom, methyl, ethyl, isopropyl and *tert*-butyl radical at the hydrogen atom in silane (SiH_4) with expulsion of silyl radical, germane (GeH_4) with expulsion of germyl radical, and the analogous reactions involving methylsilane ($MeSiH_3$), dimethylsilane (Me_2SiH_2), trimethylsilane (Me_3SiH) and trisilylsilane [$(H_3Si)_3SiH$] and the analogous germanes ($MeGeH_3$, Me_2GeH_2, Me_3GeH) by *ab initio* molecular orbital theory and, for comparison in some cases, AM1 (semiempirical) calculations.

Methods

All *ab initio* molecular orbital calculations were carried out using the GAUSSIAN92[20] or GAUSSIAN94[21] programs. Geometry optimisations were performed using standard gradient techniques at the SCF and MP2 levels of theory using RHF and UHF methods for closed and open shell systems, respectively.[22] Further single-point QCISD calculations were performed on most of the MP2 optimised structures; some QCISD calculations were beyond our resources. When correlated methods were used calculations were performed using the frozen core approximation. Vibrational frequencies were calculated on each SCF-calculated structure and at the MP2 level on the reactants, products and transition states involved in the reaction of hydrogen atom and methyl radical with silane (SiH_4) and germane (GeH_4). Where appropriate, zero-point vibrational energy (ZPE) corrections have been applied.

All *ab initio* calculations were performed using the previously published DZP basis set[11–14] on a Sun SparcStation 5, Cray Y-MP4E/364 or Cray J916 computer.

AM1 and AM1 (CI = 2) calculations were performed within GAUSSIAN92 or AMPAC 5.0[23] on a Sun SparcStation 2 or Sun SparcStation 5.

Results and discussion

Reaction involving hydrogen atom

Species of C_{3v} symmetry (**1**, **4**, **5**) were located on the SiH_5, Me_3SiH_2 and $(H_3Si)_3SiH_2$ potential energy surfaces at the SCF/DZP and MP2/DZP levels of theory, while structures of C_s symmetry (**2**, **3**) were located on the $MeSiH_4$ and Me_2SiH_3 energy surfaces. These structures were found to correspond to the transition states for transfer of hydrogen atom from the silicon centre to hydrogen atom (Scheme 1; Y = H_3Si; R = H) and are

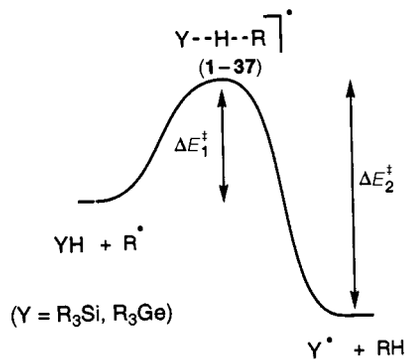

Scheme 1

displayed in Fig. 1, while the calculated energy barriers for these reactions are listed in Table 1 together with the calculated (imaginary) stretching frequency associated with the reaction coordinate in each case. Calculated energies of all structures in this study are listed in Table 2, while full geometries are available as supplementary material (SUPPL. NO. 57341, 15 pp.). For details of the Supplementary Publications Scheme see 'Instructions for Authors', *J. Chem. Soc.*, *Perkin Trans. 2*, available *via* the RSC Web page (http://www.rsc.org/authors).

The data displayed in Table 1 reveal calculated energy barriers of 80.2 (SCF/DZP), 48.4 (MP2/DZP) and 35.5 kJ mol^{-1} (QCISD/DZP//MP2/DZP) for the abstraction of a hydrogen atom from silane ($\Delta E_1^{\ddagger}$) with barriers for the reverse reaction ($\Delta E_2^{\ddagger}$) of 102.0, 96.5 and 97.7 kJ mol^{-1} at increasing levels of theory respectively. Inclusion of zero-point vibrational energy correction (ZPE) serves to lower slightly the forward barriers ($\Delta E_1^{\ddagger}$) by a maximum of 3.0 kJ mol^{-1}, while the reverse barriers ($\Delta E_2^{\ddagger}$) are also lowered by 3.6–4.0 kJ mol^{-1}. The QCISD/DZP//MP2/DZP energy barrier for the attack of a hydrogen

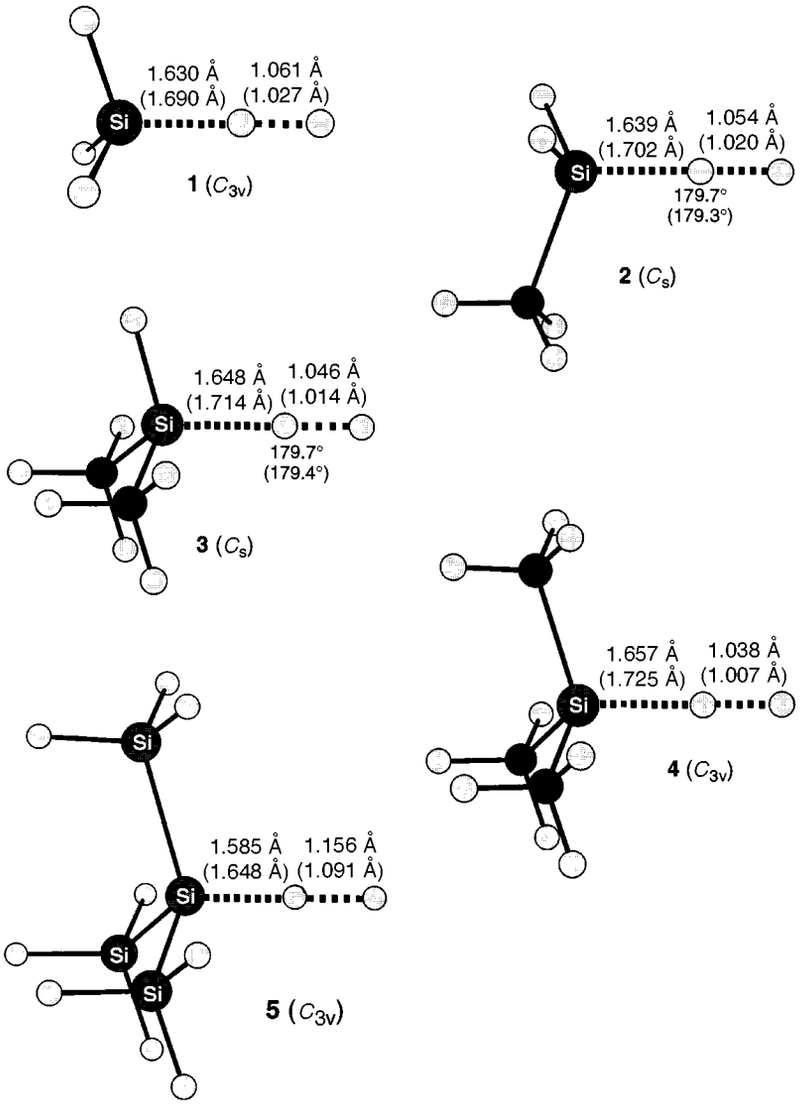

Fig. 1 MP2/DZP calculated transition states (**1**–**5**) (SCF data in parentheses) for hydrogen abstraction by hydrogen atoms from silane, methylsilane, dimethylsilane, trimethylsilane and trisilylsilane

atom at silane compares favourably with the CISD + SCC/6-31G**//HF/6-31G* value of 32.2 kJ mol^{-1};[15] similar agreement is found for the reverse barriers ($\Delta E_2^{\ddagger}$) (QCISD/DZP: 97.7 kJ mol^{-1}; CISD + SCC/6-31G**: 91.6 kJ mol^{-1}).

The SCF/DZP calculated geometry of **1**, with an H–H distance of 1.027 Å and C–H_{TS} distance of 1.690 Å is similar to the HF/6-31G** calculated transition state, with values of 1.008 and 1.708 Å for the same two parameters as reported by Tachibana *et al.*[15] Inclusion of electron correlation serves to increase the 'earliness' of transition state **1**, with calculated H–H and C–H_{TS} separations of 1.061 and 1.063 Å respectively.

The SCF/DZP and MP2/DZP calculated geometries of silane (SiH_4) and silyl radical ($^{\bullet}SiH_3$) are to be compared with experimental and other previously calculated data. Values for the Si–H separation in SiH_4 (T_d) of 1.466 and 1.468 Å at the higher and lower levels of theory respectively are in good agreement with the HF/6-31G* value[15] and somewhat shorter than the JMW/DND (density functional) value of 1.498 Å.[17] In addition, the silyl radical is calculated at SCF/DZP and MP2/DZP levels to have an Si–H separation of 1.466 (MP2) and 1.468 Å (SCF) and an H–Si–H angle of 107.4 (MP2) and 107.7° (SCF). These data are to be compared with those obtained using HF/6-31G*,[15] JMW/DND (1.502 Å, 110.4°)[17] and a double-ζ (all-electron) basis set (1.477 Å, 111.2°),[16] as well as experimental data which provide an H–Si–H angle of between 107.2 and 115.1°.[8]

It is interesting to note that increasing methyl substitution on silicon in moving from silane to trimethylsilane has little effect on the barrier for the forward reaction ($\Delta E_1^{\ddagger}$) at correlated levels, with slight reductions in the reverse barrier ($\Delta E_2^{\ddagger}$) of approximately 12 kJ mol^{-1} over the range of compounds at each level of theory. Overall, these reactions are predicted to be significantly exothermic at each level of theory.

The introduction of three silyl substituents in moving to trisilylsilane as the reagent has the most profound effect on the reaction profile; trisilylsilane is predicted at each level of theory to have a lower forward barrier ($\Delta E_1^{\ddagger}$) of between 26.8 (QCISD) and 54.3 (SCF) kJ mol^{-1}, in keeping with the expected 'more stannane-like' behaviour of trisilylsilane.[2,6,9]

These data are to be compared with those obtained for the analogous reactions involving stannane and trimethyltin hydride.[14] Forward barriers ($\Delta E_1^{\ddagger}$) of 20.6 and 18.1 kJ mol^{-1} are calculated at the QCISD/DZP//MP2/DZP level for the reaction of hydrogen atom with SnH_4 and $MeSnH_3$ respectively, some 15–19 kJ mol^{-1} lower than the corresponding reactions involving silane and trimethylsilane and more similar to the predictions for trisilylsilane.

Inspection of Fig. 1 reveals a pleasing level of correlation between the SCF and MP2 generated transition state structures (**1**–**4**). At the lower level, H–H separations of between 1.007 and 1.027 Å are predicted, with corresponding Si–H_{TS} separations of between 1.690 and 1.725 Å. Inclusion of electron

Table 2 SCF, MP2, QCISD,[a] AM1 and AM1 (CI = 2) calculated energies[b] of the reactants, products and transition states (**1**–**37**) in this study

Structure	SCF/DZP	MP2/DZP	QCISD/DZP	AM1[c]	AM1 (CI = 2)[c]
$H^{\bullet}$	−0.497 64	—	—	—	—
$^{\bullet}CH_3$	−39.571 76[d–g]	−39.697 27[d–g]	−39.718 91[d–g]	0.047 71[e]	0.011 90[e]
$^{\bullet}CH_2CH_3$	−78.617 06[e,g]	−78.881 30[e,g]	−78.916 95[e,g]	0.024 62[e]	0.006 91[e]
$^{\bullet}Pr^{i}$	−117.663 50[e,g]	−118.068 14[e,g]	−118.117 13[e,g]	0.005 62[e]	0.002 53[e]
$^{\bullet}Bu^{t}$	−156.710 09[e]	−157.257 30[e]	−157.318 90[e]	−0.010 31[e]	−0.001 11[e]
$^{\bullet}SiH_3$	−5.469 84[d–g]	−5.559 64[d–g]	−5.583 57[d–g]	0.009 33[e]	0.010 03[e]
$^{\bullet}SiH_2Me$	−44.524 24	−44.754 94	−44.791 27	—	—
$^{\bullet}SiHMe_2$	−83.578 84	−83.951 32	−83.999 87	—	—
$^{\bullet}SiMe_3$	−122.633 73	−123.148 87	−123.209 47	—	—
$^{\bullet}Si(SiH_3)_3$	−20.312 22[g]	−20.690 08[g]	−20.770 86[g]	—	—
$^{\bullet}GeH_3$	−5.345 97[d–g]	−5.433 46[d–g]	−5.456 94[d–g]	—	—
$^{\bullet}GeH_2Me$	−44.397 38	−44.626 77	−44.662 43	—	—
$^{\bullet}GeHMe_2$	−83.449 03	−83.821 05	−83.868 74	—	—
$^{\bullet}GeMe_3$	−122.501 08	−123.016 47	−123.076 04	—	—
Me_3SiH	−123.258 27	−123.794 78	−123.858 99	—	—
$(H_3Si)_3SiH$	−20.921 44	−21.321 08	−21.404 70	—	—
GeH_4	−5.954 99	−6.063 48	−6.090 67	—	—
$MeGeH_3$	−45.007 69	−45.257 78	−45.297 15	—	—
Me_2GeH_2	−84.060 67	−84.453 17	−84.504 59	—	—
Me_3GeH	−123.113 90	−123.649 64	−123.712 95	—	—
1	−6.562 22	−6.680 90	−6.712 04	—	—
2	−45.617 75	−45.877 66	−45.921 14	—	—
3	−84.673 53	−85.075 66	−85.131 31	—	—
4	−123.729 49	−124.274 81	−124.342 44	—	—
5	−21.398 38	−21.805 80	−21.892 15	—	—
6	−45.626 21	−45.878 88	−45.927 67	0.014 85	0.017 27
7	−84.670 58	−85.064 13	−85.126 27	0.010 23	0.012 46
8	−123.716 45	−124.252 78	−124.327 47	0.006 60	0.008 67
9	−162.762 81	−163.444 52	−163.530 89	0.003 91	0.005 85
10	−84.680 64	−85.075 04	−85.136 05	—	—
11	−123.724 67	−124.259 97	−124.334 31	—	—
12	−162.770 25	−163.448 72	—	—	—
13	−201.816 45	−202.640 33	—	—	—
14	−123.735 49	−124.272 56	—	—	—
15	−162.779 19	−163.457 56	—	—	—
16	−201.824 60	−202.645 71	—	—	—
17	−162.790 63	−163.471 33	−163.556 22	—	—
18	−201.834 07	−202.656 06	—	—	—
19	−60.462 85	−61.005 15	−61.109 32	—	—
20	−99.507 63	−100.191 71	—	—	—
21	−6.432 62	−6.547 31	−6.577 51	—	—
22	−45.497 00	−45.745 21	−45.793 71	—	—
23	−84.541 61	−84.930 70	−84.992 04	—	—
24	−123.587 67	−124.119 50	−124.193 89	—	—
25	−162.634 19	−163.311 35	−163.397 45	—	—
26	−45.485 28	−45.741 99	−45.784 31	—	—
27	−84.548 47	−84.939 17	−84.999 73	—	—
28	−123.592 78	−124.124 40	−124.198 29	—	—
29	−162.638 60	−163.313 28	−163.399 66	—	—
30	−201.684 97	−202.505 00	—	—	—
31	−84.538 20	−84.937 77	−84.992 08	—	—
32	−123.600 36	−124.134 36	—	—	—
33	−162.644 39	−163.319 62	—	—	—
34	−201.690 03	−202.508 07	—	—	—
35	−123.591 36	−124.134 70	−124.200 85	—	—
36	−162.652 61	−163.330 81	−163.415 06	—	—
37	−201.696 39	−202.515 90	—	—	—

[a] QCISD/DZP//MP2/DZP. [b] Energies in hartrees (1 E_h = 2626 kJ mol^{-1}). [c] Heat of formation. [d] Ref. 12. [e] Ref. 14. [f] Ref. 11. [g] Ref. 25.

correlation (MP2) serves to alter the position of the transferring hydrogen atom in each transition state without significantly altering the overall gross transition state structure, H–H separations of between 1.038 and 1.061 Å coupled with Si–H_{TS} distances of between 1.630 and 1.657 Å lead to overall Sn–H_{attack} distances of between 2.691 and 2.695 Å at the MP2/DZP level of theory. These distances are slightly shorter than those calculated at the SCF level of theory, namely 2.717– 2.732 Å.

Reaction of methyl, ethyl, isopropyl and *tert*-butyl radicals with silane (SiH_4)

Extensive searching of the potential energy surfaces for the hydrogen atom transfer reactions involving silane and methyl, ethyl, isopropyl and *tert*-butyl radicals (Scheme 1; Y = H_3Si; R ≠ H) located structures **6**–**9** as stationary points at each level of theory. These structures proved to be transition states for the transfer of hydrogen atom and were found to adopt colinear arrangements of attacking and leaving radicals (C_{3v} symmetry) in reactions involving methyl and *tert*-butyl radicals (**6**, **9**). In the remaining cases (**7**, **8**), slight deviations from colinearity are predicted (C_s symmetry) with Sn–H_{TS}–C angles ranging from 175.9 to 178.6°. The MP2/DZP calculated transition structures are shown in Fig. 2.

Ab initio calculated energy barriers for these hydrogen atom transfer reactions ($\Delta E_1^{\ddagger}$, $\Delta E_2^{\ddagger}$, Scheme 1) are listed in Table 3, while the calculated energies of all structures in this study are found in Table 2. AM1 generated data are included for comparison with our previous AM1 calculations involving stannanes.[14]

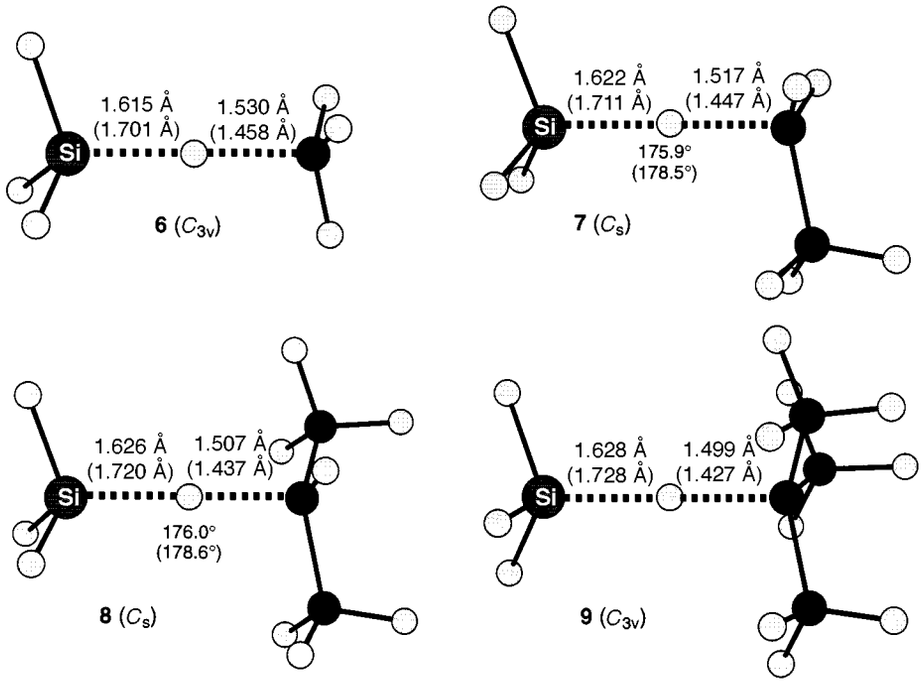

Fig. 2 MP2/DZP calculated transition states (**6**–**9**) (SCF data in parentheses) for hydrogen abstraction by methyl, ethyl, isopropyl and *tert*-butyl radicals from silane

Table 3 Calculated energy barriers[a] for the forward ($\Delta E_1^{\ddagger}$) and reverse ($\Delta E_2^{\ddagger}$) hydrogen atom abstraction reactions of methyl, ethyl, isopropyl and *tert*-butyl radicals with silane (SiH_4) (Scheme 1, Y = H_3Si) and transition state (imaginary) frequency (ν)[b] of structures **6**–**9**

R	TS	Method	$\Delta E_1^{\ddagger}$	$\Delta E_1^{\ddagger}$ + ZPVE[c]	$\Delta E_2^{\ddagger}$	$\Delta E_1^{\ddagger}$ + ZPVE[c]	ν
Me	**6**	SCF/DZP	94.7	99.2	134.3	122.0	2088i
		MP2/DZP	52.8	54.2	125.4	113.0	1538i
		QCISD/DZP[d]	50.7	[52.1]	119.2	[106.8]	—
		AM1	20.5	—	97.5	—	836i
		AM1 (CI = 2)	43.8	—	119.6	—	1429i
Et	**7**	SCF/DZP	97.1	99.9	126.7	112.9	2080i
		MP2/DZP	49.6	(52.7)	112.7	(98.9)	—
		QCISD/DZP[d]	49.2	(52.0)	107.1	(93.3)	—
		AM1	30.3	—	82.8	—	1121i
		AM1 (CI = 2)	45.9	—	100.5	—	1466i
Pr^i	**8**	SCF/DZP	98.6	99.7	119.4	104.8	2057i
		MP2/DZP	44.8	(45.9)	100.6	(86.0)	—
		QCISD/DZP[d]	46.5	(47.6)	95.7	(81.1)	—
		AM1	41.2	—	71.6	—	1362i
		AM1 (CI = 2)	53.4	—	87.4	—	1520i
Bu^t	**9**	SCF/DZP	99.2	98.7	112.2	97.2	2029i
		MP2/DZP	38.0	(37.5)	88.6	(73.6)	—
		QCISD/DZP[d]	42.2	(41.7)	84.7	(69.7)	—
		AM1	52.5	—	63.4	—	1540i
		AM1 (CI = 2)	61.3	—	78.4	—	1598i

[a] Energies in kJ mol^{-1}. [b] Frequencies in cm^{-1}. [c] Values in parentheses are estimates based on SCF/DZP ZPE corrections. Values in square brackets are estimates based on MP2/DZP ZPE corrections. [d] QCISD/DZP//MP2/DZP.

Inspection of Table 3 reveals a pleasing level of convergence in the forward energy barriers ($\Delta E_1^{\ddagger}$). For example, attack of methyl radical at silane is predicted to have associated barriers of 94.7 (SCF/DZP), 52.8 (MP2/DZP) and 50.7 kJ mol^{-1} (QCISD/DZP//MP2/DZP), suggesting that the MP2 level of theory is able to provide acceptable data; improvement in the level of correlation has only a minor effect on $\Delta E_1^{\ddagger}$. Similar convergence is observed for reactions involving ethyl, isopropyl and *tert*-butyl radicals, with QCISD calculated values of $\Delta E_1^{\ddagger}$ lying within 4.2 kJ mol^{-1} of the corresponding MP2 value.

All reactions are predicted to be significantly exothermic, with reverse barriers ($\Delta E_2^{\ddagger}$) ranging from 84.7 (**9**) to 119.2 kJ mol^{-1} (**6**) at the QCISD level. As was observed for reactions involving a hydrogen atom, zero-point vibrational energy correction (ZPE) leads to slight changes (−0.5 to 4.5 kJ mol^{-1}) in the predicted values of $\Delta E_1^{\ddagger}$, while the reverse reactions ($\Delta E_2^{\ddagger}$) are affected more strongly (−12 to −15 kJ mol^{-1}).

Comparing these data with those for hydrogen abstraction by various alkyl radicals from stannane,[14] as expected, reveals the reactions of stannane to be more facile, with QCISD/DZP// MP2/DZP calculated energy barriers of between 18.7 and 33.9 kJ mol^{-1}.

Inspection of Fig. 2 reveals that the overall structures of transition states **6**–**9** are only slightly affected by substitution at the carbon radical centre at both SCF/DZP and MP2/DZP levels of theory. Overall Si–C distances lie between 3.127 and 3.145 Å (MP2). As was observed for the analogous reactions

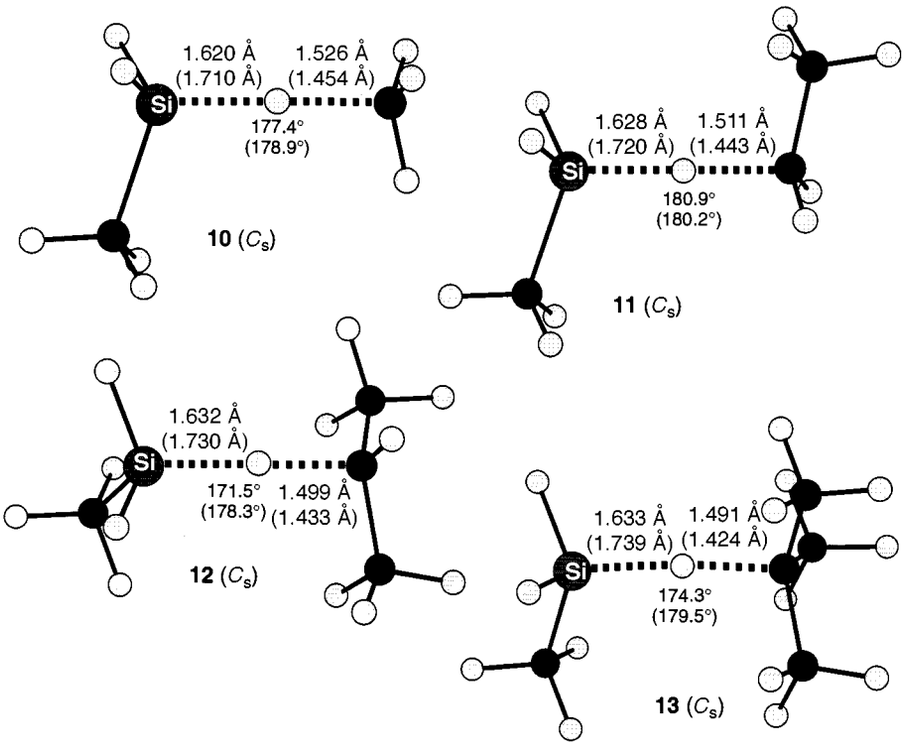

Fig. 3 MP2/DZP calculated transition states (**10**–**13**) (SCF data in parentheses) for hydrogen abstraction by methyl, ethyl, isopropyl and *tert*-butyl radicals from methylsilane

involving stannane,[14] the greatest effect appears to be on the absolute position of the hydrogen atom in the transition state during delivery. For example, at the MP2 level of theory, the Si–H_{TS} separation is found to vary between 1.615 (Me) and 1.628 Å (*tert*-butyl) while the C–H_{TS} distance is predicted to lie in the range 1.530 (Me)–1.499 Å (*tert*-butyl). In other words, the transition state becomes 'earlier' in moving from methyl through to *tert*-butyl as the attacking radical. This trend is consistent with the decreases in (forward) energy barrier observed in moving from methyl (50.7 kJ mol^{-1}) to *tert*-butyl (42.4 kJ mol^{-1}). Similar trends are predicted for reactions involving stannane.[14]

In order to make comparisons with our previous work,[14] AM1 and AM1 (CI = 2) calculations were also performed on reactions involving silane. These calculations predict similar transition state geometries to those calculated using *ab initio* techniques, the major differences being in Si–H_{TS} and C–H_{TS} distances which fall in the range 1.519–1.595 and 1.530–1.650 Å respectively.† These data are consistent with 'earlier' transition states when AM1 is employed. The AM1 calculated energy barriers ($\Delta E_1^{\ddagger}$, $\Delta E_2^{\ddagger}$) are also of interest. Table 3 clearly reveals the AM1 calculated trends in $\Delta E_1^{\ddagger}$. Values of 20.5, 30.3, 41.2 and 52.5 kJ mol^{-1} are predicted for reactions involving transition states **6**–**9** respectively. In other words, in moving from methyl radical to primary, secondary and tertiary radicals as hydrogen abstracting species, the energy barrier ($\Delta E_1^{\ddagger}$) is predicted to undergo increases of up to 32 kJ mol^{-1}. Similar predictions are made by AM1 for the analogous reactions involving stannane.

It is interesting to compare these data with those calculated using *ab initio* techniques. While SCF/DZP calculations suggest that $\Delta E_1^{\ddagger}$ is about 94–99 kJ mol^{-1} in all cases, inclusion of electron correlation results in decreases in $\Delta E_1^{\ddagger}$ in moving through the same set of hydrogen abstracting radicals. Barriers of 50.7, 49.2, 46.5 and 42.2 kJ mol^{-1} are predicted at the QCISD/DZP//MP2/DZP level for reactions involving transition states **6**–**9** respectively. Unfortunately, experimentally determined activation energies are unavailable for reactions of alkyl radicals with silane, however, trends observed for substituted silanes (*vide infra*) would suggest that the trends predicted by SCF/DZP and AM1 for reactions involving SiH_4 are incorrect and that electron correlation is required to provide reliable data. Unfortunately, the data generated by AM1 (CI = 2) would also appear to be unreliable, an observation supported by previous calculations.[14]

Reaction of methyl, ethyl, isopropyl and *tert*-butyl radicals with methylsilane ($MeSiH_3$) and dimethylsilane (Me_2SiH_2)

Structures **10**–**16** of C_s symmetry were located on the SCF/DZP and MP2/DZP potential energy surfaces for the reactions of alkyl radicals with methylsilane and dimethylsilane; these structures proved to correspond to transition states for the delivery of hydrogen atom from the silane to the alkyl radical. Further QCISD/DZP single-point energy refinements were only carried out on structures **10** and **11**, while location of the transition state for the reaction of *tert*-butyl radical with dimethylsilane and QCISD/DZP calculations on **12** and **13** proved to be tasks beyond our current resources.

The MP2/DZP calculated transition structures (**10**–**16**) are displayed in Figs. 3 and 4, while the calculated energy barriers ($\Delta E_1^{\ddagger}$, $\Delta E_2^{\ddagger}$) for these reactions are listed in Tables 4 and 5. Comparison of the data presented in these tables with those in Table 3 and Fig. 2 reveal the marginal effect that alkyl substitution at silicon has on both transition state geometry and activation energy for a given (attacking) alkyl radical. For example, Si–H_{TS} and C–H_{TS} separations in transition states **6**, **10** and **14** all lie in the narrow range 1.615–1.624 and 1.521–1.530 Å respectively at the MP2/DZP level of theory. Analogous similarities are observed between **7**, **11** and **15** as well as between **7**, **12** and **16**.

† AM1 calculated geometries for **6**–**9** are: r(Si–H_{TS}) = 1.539 (Me), 1.556 (Et), 1.575 (Pr^i), 1.595 Å (Bu^t); r(C–H_{TS}) = 1.630 (Me), 1.587 (Et), 1.552 (Pr^i), 1.530 Å (Bu^t); θ = 180 (Me), 178.3 (Et), 178.1 (Pr^i), 180° (Bu^t). AM1 (CI = 2) calculated geometries for **6**–**9** are: r(Si–H_{TS}) = 1.519 (Me), 1.535 (Et), 1.552 (Pr^i), 1.571 Å (Bu^t); r(C–H_{TS}) = 1.650 (Me), 1.617 (Et), 1.588 (Pr^i), 1.563 Å (Bu^t); θ = 180 (Me), 179.3 (Et), 178.7 (Pr^i), 180° (Bu^t).

Table 4 Calculated energy barriers[a] for the forward ($\Delta E_1^{\ddagger}$) and reverse ($\Delta E_2^{\ddagger}$) hydrogen atom abstraction reactions of methyl, ethyl, isopropyl and *tert*-butyl radicals with methylsilane ($MeSiH_3$) (Scheme 1, Y = MeH_2Si) and transition state (imaginary) frequency (ν)[b] of structures **10**–**13**

R	TS	Method	$\Delta E_1^{\ddagger}$	$\Delta E_1^{\ddagger}$ + ZPVE[c]	$\Delta E_2^{\ddagger}$	$\Delta E_1^{\ddagger}$ + ZPVE[c]	ν
Me	**10**	SCF/DZP	98.1	100.5	134.2	120.4	2113i
		MP2/DZP	53.8	(56.2)	123.2	(109.4)	—
		QCISD/DZP[d]	55.2	(57.6)	117.4	(103.6)	—
Et	**11**	SCF/DZP	101.4	105.9	127.5	112.1	2116i
		MP2/DZP	51.4	(55.9)	111.3	(95.9)	—
		QCISD/DZP[d]	54.7	(59.2)	106.2	(90.8)	—
Pr^i	**12**	SCF/DZP	103.6	102.5	121.0	104.9	2106i
		MP2/DZP	46.3	(45.2)	98.9	(82.8)	—
Bu^t	**13**	SCF/DZP	104.7	100.4	114.2	96.2	2085i
		MP2/DZP	39.9	(35.6)	87.2	(69.2)	—

[a] Energies in kJ mol^{-1}. [b] Frequencies in cm^{-1}. [c] Values in parentheses are estimates based on SCF/DZP ZPE corrections. [d] QCISD/DZP//MP2/DZP.

Table 5 Calculated energy barriers[a] for the forward ($\Delta E_1^{\ddagger}$) and reverse ($\Delta E_2^{\ddagger}$) hydrogen atom abstraction reactions of methyl, ethyl, isopropyl and *tert*-butyl radicals with dimethylsilane (Me_2SiH_2) (Scheme 1, Y = Me_2HSi) and transition state (imaginary) frequency (ν)[b] of structures **14**–**16**

R	TS	Method	$\Delta E_1^{\ddagger}$	$\Delta E_1^{\ddagger}$ + ZPVE[c]	$\Delta E_2^{\ddagger}$	$\Delta E_1^{\ddagger}$ + ZPVE[c]	ν
Me	**14**	SCF/DZP	100.9	103.1	133.6	118.8	2126i
		MP2/DZP	54.3	(56.5)	120.2	(105.4)	—
Et	**15**	SCF/DZP	105.1	105.5	127.7	111.4	2142i
		MP2/DZP	51.8	(52.2)	108.1	(91.8)	—
Pr^i	**16**	SCF/DZP	107.8	106.4	121.6	104.4	2137i
		MP2/DZP	48.3	(46.9)	97.2	(80.0)	—

[a] Energies in kJ mol^{-1}. [b] Frequencies in cm^{-1}. [c] Values in parentheses are estimates based on SCF/DZP ZPE corrections. [d] QCISD/DZP//MP2/DZP.

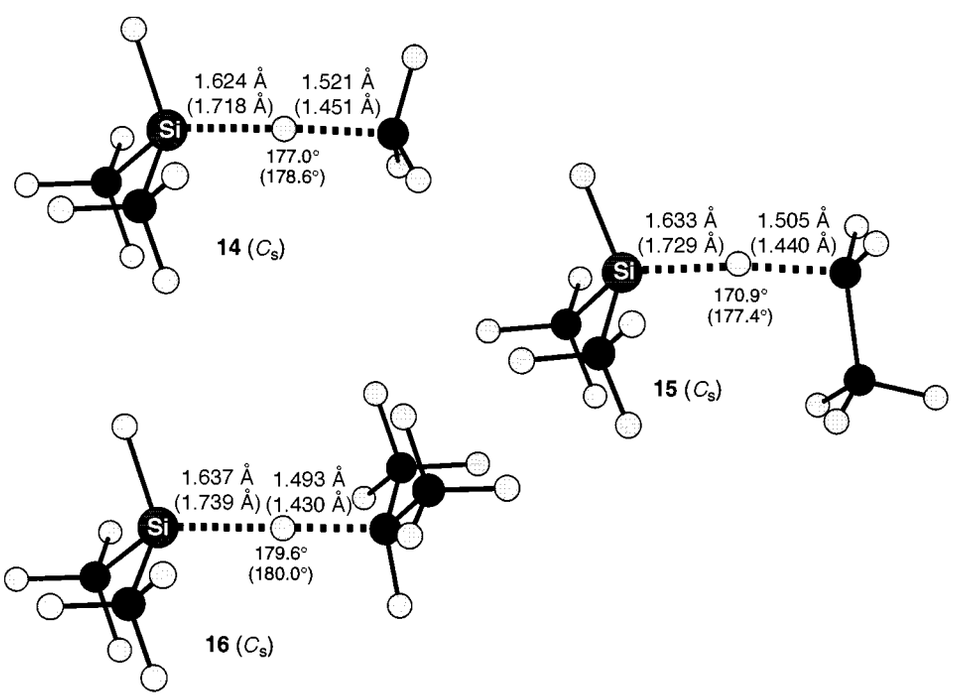

Fig. 4 MP2/DZP calculated transition states (**14**–**16**) (SCF data in parentheses) for hydrogen abstraction by methyl, ethyl and isopropyl radicals from dimethylsilane

While slight increases in $\Delta E_1^{\ddagger}$ are predicted at the SCF/DZP level as alkyl substitution at silicon is increased in reactions involving a given radical, the MP2/DZP data indicate that these forward barriers all lie in a narrow range, with only very slight increases with increased substitution. For example, the reactions involving methyl radical are calculated to have $\Delta E_1^{\ddagger}$ values of 52.8 (SiH_4), 53.5 ($MeSiH_3$) and 54.3 kJ mol^{-1} (Me_2SiH_2) at the MP2/DZP level. Similar insensitivities toward silicon substitution are predicted for reactions involving other alkyl radicals, with MP2/DZP calculated barriers of 49.9–51.8 (Et), 44.8–48.3 (Pr^i) and 38.0–(*ca.*) 40 kJ mol^{-1} (Bu^t). Similar trends are observed in the reverse barriers ($\Delta E_2^{\ddagger}$).

Reaction of methyl and ethyl radicals with trimethylsilane (Me_3SiH) and trisilylsilane [$(H_3Si)_3SiH$]

Structures of C_{3v} (**17**, **19**) and C_s (**18**, **20**) symmetry were located on the SCF/DZP and MP2/DZP potential energy surfaces for

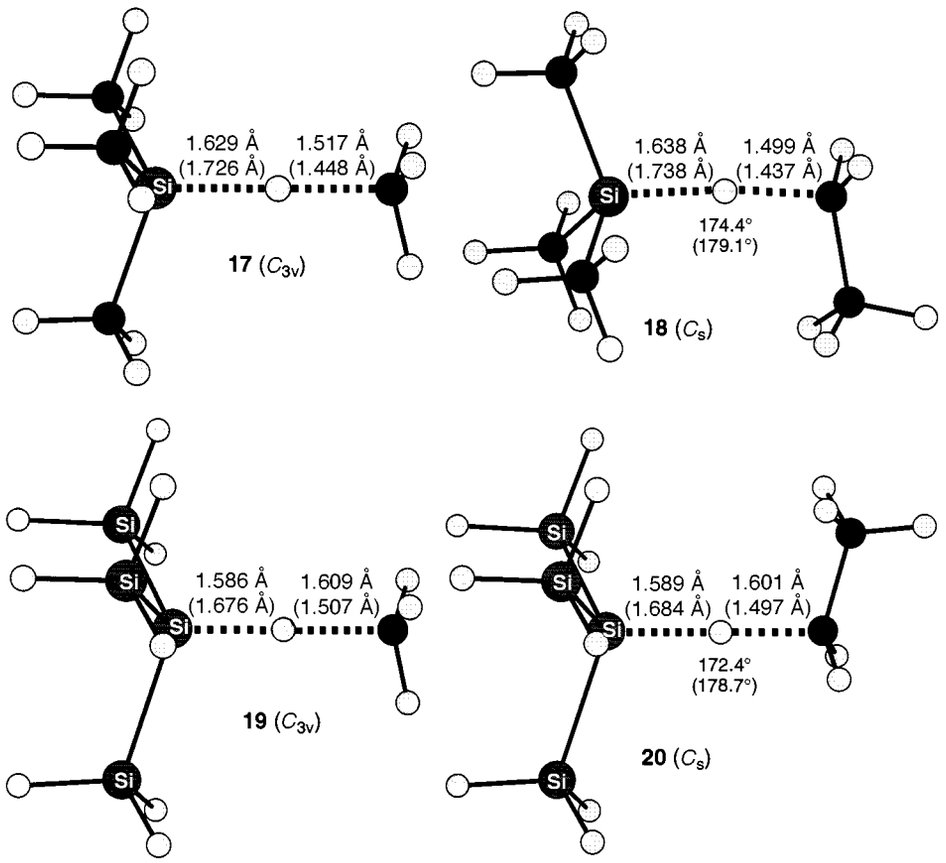

Fig. 5 MP2/DZP calculated transition states (**17**–**20**) (SCF data in parentheses) for hydrogen abstraction by methyl and ethyl radicals from trimethylsilane and trisilylsilane

Table 6 Calculated energy barriers[a] for the forward ($\Delta E_1^{\ddagger}$) and reverse ($\Delta E_2^{\ddagger}$) hydrogen atom abstraction reactions of methyl, ethyl and isopropyl with dimethylsilane (Me_2SiH_2), trimethylsilane (Me_3SiH) and trisilylsilane [$(H_3Si)_3SiH$] (Scheme 1) and transition state (imaginary) frequency (ν)[b] of structures **17**–**20**

Y	R	TS	Method	$\Delta E_1^{\ddagger}$	$\Delta E_1^{\ddagger}$ + ZPVE[c]	$\Delta E_2^{\ddagger}$	$\Delta E_1^{\ddagger}$ + ZPVE[c]	ν
Me_3Si	Me	**17**	SCF/DZP	103.5	106.7	132.9	117.6	2134i
			MP2/DZP	54.4	(57.6)	117.0	(101.7)	—
			QCISD/DZP[d]	56.9	(60.1)	112.2	(96.9)	—
Me_3Si	Et	**18**	SCF/DZP	108.3	109.9	127.8	110.9	2158i
			MP2/DZP	52.6	(53.9)	105.6	(88.7)	—
$(H_3Si)_3Si$	Me	**19**	SCF/DZP	79.7	82.6	149.4	132.5	1973i
			MP2/DZP	34.6	(37.5)	136.4	(119.5)	—
			QCISD/DZP[d]	37.5	(40.6)	134.0	(117.1)	—
$(H_3Si)_3Si$	Et	**20**	SCF/DZP	81.0	82.0	140.7	122.2	1964i
			MP2/DZP	28.0	(29.0)	120.2	(101.7)	—

[a] Energies in kJ mol^{-1}. [b] Frequencies in cm^{-1}. [c] Values in parentheses are estimates based on SCF/DZP ZPE corrections. [d] QCISD/DZP//MP2/DZP.

reactions of trimethylsilane and trisilylsilane with methyl and ethyl radicals respectively. The structures proved to correspond to the expected hydrogen transfer transition states. Resource restrictions deemed that the modelling of reactions involving isopropyl and *tert*-butyl radicals and QCISD (single-point) calculations on **18** and **20** were tasks requiring unacceptable amounts of computing resources.

Transition states **17**–**20** are displayed in Fig. 5, while the energy barriers ($\Delta E_1^{\ddagger}$, $\Delta E_2^{\ddagger}$) for the forward and reverse hydrogen abstractions reactions [Scheme 1, Y = Me_3Si, $(H_3Si)_3Si$] are listed in Table 6. Inspection of the data presented reveals, once again, that the transition states (**17**, **18**) for reactions involving trimethylsilane are very similar in geometry to those calculated for the other reactions involving methyl and ethyl radicals; both **17** and **18** are predicted to be slightly 'later' than the similar transition states involving SiH_4, $MeSiH_3$ and Me_2SiH_2. The overall Si–C_{attack} distances of 3.146 (**17**) and 3.137 Å (**18**) calculated at the MP2/DZP level are very similar to those calculated for the other transition states in this study (*vide supra*).

As expected from the trends already observed, the forward barrier ($\Delta E_1^{\ddagger}$) is predicted at the MP2/DZP level of theory, at 54.4 and 52.6 kJ mol^{-1} to be slightly higher than the analogous reactions involving the other silanes in this study. These values are to be compared with the experimentally determined activation energy for the hydrogen abstraction by primary alkyl radical from triethylsilane of 33.5 kJ mol^{-1}.[9] Our calculations provide values some 20 kJ mol^{-1} higher than the experimental value. Similar discrepancies were observed for reactions involving stannanes and were attributed to possible solvent effects, stannane substitution or tunelling.[14]

Table 7 Important geometric features[a] of transition states **21**–**35** (Scheme 1; Y = R_3Ge)

			r(Ge–H_{TS})		r(C–H_{TS})		θ(Ge–H_{TS}–C)	
Y	R	TS	SCF/DZP	MP2/DZP	SCF/DZP	MP2/DZP	SCF/DZP	MP2/DZP
H_3Ge	H	**21**	1.704	1.648	1.104	1.157	180.0	180.0
H_3Ge	Me	**22**	1.733	1.653	1.514	1.602	180.0	180.0
H_3Ge	Et	**23**	1.741	1.658	1.503	1.590	178.4	175.8
H_3Ge	Pr^i	**24**	1.748	1.660	1.439	1.582	178.5	175.7
H_3Ge	Bu^t	**25**	1.755	1.659	1.484	1.579	180.0	180.0
MeH_2Ge	H	**26**	1.711	1.653	1.097	1.154	180.0	180.0
MeH_2Ge	Me	**27**	1.741	1.657	1.510	1.598	179.3	178.7
MeH_2Ge	Et	**28**	1.750	1.663	1.498	1.584	180.8	182.8
MeH_2Ge	Pr^i	**29**	1.758	1.665	1.488	1.575	178.1	171.2
MeH_2Ge	Bu^t	**30**	1.765	1.664	1.478	1.571	179.5	175.1
MeH_2Ge	H	**31**	1.720	1.657	1.090	1.152	180.2	179.8
MeH_2Ge	Me	**32**	1.748	1.661	1.505	1.595	179.0	178.5
MeH_2Ge	Et	**33**	1.758	1.667	1.493	1.579	177.4	171.5
MeH_2Ge	Pr^i	**34**	1.766	1.670	1.483	1.568	179.4	177.4
Me_3Ge	H	**35**	1.728	1.661	1.082	1.149	180.0	180.0
Me_3Ge	Me	**36**	1.756	1.665	1.501	1.592	180.0	180.0
Me_3Ge	Et	**37**	1.767	1.672	1.489	1.574	181.2	186.0

[a] Distances in Å; angles (θ) in degrees.

Introduction of silyl substitution at silicon has a profound effect on both transition state geometry and reaction profile. Inspection of Fig. 5 reveals significantly 'earlier' transition states (**19**, **20**) with MP2/DZP calculated Si–H_{TS} separations of 1.586 and 1.589 Å for reactions involving methyl and ethyl radicals respectively, while the C–H_{TS} distances are predicted to be 1.609 (Me) and 1.601 Å (Et) at the same level of theory. These geometric changes are consistent with the substantially reduced (forward) energy barriers ($\Delta E_1^{\ddagger}$) calculated at both MP2 and QCISD levels. Values of $\Delta E_1^{\ddagger}$ of 37.5 and 28.0 kJ mol^{-1} are predicted at the MP2/DZP level for the reactions of trisilylsilane with methyl and ethyl radicals respectively. These numbers can be compared with the experimentally determined activation energies for the reactions of TTMSS with primary (18.8 kJ mol^{-1}), secondary (18.0 kJ mol^{-1}) and tertiary (14.2 kJ mol^{-1}) radicals.[9] Once again, calculated and experimental data diverge by some 9 kJ mol^{-1}; divergences of some 7–18 kJ mol^{-1} were observed in our previous stannane work. We have demonstrated previously that the silyl substituent is a poor model for the trimethylsilyl group in calculations involving carbocations;[24] we speculate that, in addition to the already discussed reasons for the differences between experimental and computational data, SiH_3 may also model TMS poorly in the calculations in this study.

Interestingly, trisilylsilane is predicted to react with methyl radical with energy barriers more similar to those calculated for trimethyltin hydride (33.0 kJ mol^{-1}) than trimethylsilane (54.4 kJ mol^{-1}) at the MP2/DZP level of theory, clearly highlighting the stannane-like behaviour of trisilylated silanes, like TTMSS.

Reactions involving germane (GeH_4), methylgermane ($MeGeH_3$), dimethylgermane (Me_2GeH_2) and trimethylgermane (Me_3GeH)

Extensive searching of the potential energy surfaces for the reactions of hydrogen atom, methyl, ethyl, isopropyl and *tert*-butyl radicals with germane (GeH_4), methylgermane ($MeGeH_3$), dimethylgermane (Me_2GeH_2) and trimethylgermane (Me_3GeH) located structures **21**–**37** as stationary points. Upon analysis of the vibrational frequencies associated with structures **21**–**37**, these proved to correspond to the transition states for the transfer of hydrogen atom from the germane to the attacking radical. SCF/DZP and MP2/DZP calculated structures (**21**–**37**) are available as supplementary material; important geometric parameters are summarised in Table 7, while the calculated energy barriers ($\Delta E_1^{\ddagger}$, $\Delta E_2^{\ddagger}$) for the forward and reverse reactions (Scheme 1, Y = R_3Ge) are listed in Table 8, together with the calculated (imaginary) stretching frequency associated with the reaction coordinate where calculated. Calculated energies of all structures in this study are listed in Table 2.

Not surprisingly the transition states for hydrogen abstraction from the various germanes in this study bear a striking similarity to the analogous transition states for hydrogen abstraction from similar silanes and stannanes.[14] Transition states are predicted to adopt colinear (or nearly so) arrangements of attacking and leaving radicals and are of either C_{3v} or C_s symmetry. The largest deviation from colinearity is predicted to involve an attack angle of 171.2° at the MP2/DZP level of theory (**29**), with the majority of angles lying within a few degrees of colinearity.

All transition states are predicted to be 'earlier' at the MP2/DZP level, consistent with higher energy barriers predicted in the absence of electron correlation (*vide infra*). For example, for reactions involving alkyl radicals, C–H_{TS} and Ge–H_{TS} distances are predicted to lie between 1.478–1.598 and 1.741–1.767 Å respectively at the lower level, while MP2/DZP calculations result in values of 1.571–1.598 and 1.653–1.672 Å for the same two parameters respectively. Interestingly, MP2/DZP calculations predict the overall Ge–C_{attack} distance to lie in the narrow range of between 3.24 and 3.26 Å for all alkyl radicals, regardless of the germane involved; the major influence of alkyl substitution on both radical centre and germanium appears to be on the exact position of the hydrogen undergoing translocation in the transition state. Similar results were obtained for analogous silicon (*vide supra*) and tin calculations.[14]

All reactions depicted in Scheme 1 (Y = R_3Ge) are calculated to be significantly exothermic. Inspection of Table 8 reveals that, as expected, the calculated energy barriers for all reactions lie somewhere between the results obtained for the analogous reactions involving silanes (*vide supra*) and stannanes[14] at the same level of theory. Once again, a zero-point vibrational energy correction affects the forward barriers ($\Delta E_1^{\ddagger}$, Scheme 1, Y = R_3Ge) by a maximum of 4.8 kJ mol^{-1}, while the barrier for the reverse reaction ($\Delta E_1^{\ddagger}$) is affected to a greater degree, with the reaction of dimethylgermyl radical with propane (transition state **34**) affected by the maximum value of 18.6 kJ mol^{-1}.

In previous calculations we noted that inclusion of electron correlation was crucial in predicting the correct order of relative reactivity of primary, secondary and tertiary radicals to abstraction of hydrogen from silanes (*vide supra*) and stannanes.[14] In the current work it is, once again, clear that SCF/DZP calculations predict forward energy barriers which are significantly too high. For example, energy barriers of 81.4, 84.0, 85.6 and 86.2 kJ mol^{-1} are predicted at the SCF/DZP level for the reactions of methyl, ethyl, isopropyl and *tert*-butyl

Table 8 Calculated energy barriers[a] for the forward ($\Delta E_1^{\ddagger}$) and reverse ($\Delta E_2^{\ddagger}$) hydrogen atom abstraction reactions of hydrogen atom and various alkyl radicals with germane (GeH_4), methylgermane ($MeGeH_3$), dimethylgermane (Me_2GeH_2) and trimethylgermane (Me_3GeH) (Scheme 1) and transition state (imaginary) frequency (ν)[b] of structures **21**–**37**

Y	R	TS	Method	$\Delta E_1^{\ddagger}$	$\Delta E_1^{\ddagger}$ + ZPVE[c]	$\Delta E_2^{\ddagger}$	$\Delta E_1^{\ddagger}$ + ZPVE[c]	ν
H_3Ge	H	**21**	SCF/DZP	52.5	49.3	117.1	112.1	1979i
			MP2/DZP	36.2	33.9	116.0	111.4	1664i
			QCISD/DZP[d]	28.3	[26.0]	118.4	[113.8]	—
H_3Ge	Me	**22**	SCF/DZP	78.1	81.2	148.3	134.5	1923i
			MP2/DZP	40.8	42.4	145.1	131.2	1278i
			QCISD/DZP[d]	41.7	[43.3]	138.4	[124.5]	—
H_3Ge	Et	**23**	SCF/DZP	79.9	81.3	140.1	124.9	1923i
			MP2/DZP	36.9	(38.3)	131.7	(116.5)	—
			QCISD/DZP[d]	40.9	(42.3)	127.0	(111.8)	—
H_3Ge	Pr^i	**24**	SCF/DZP	80.9	80.6	132.3	116.2	1908i
			MP2/DZP	31.8	(31.5)	119.2	(103.2)	—
			QCISD/DZP[d]	36.5	(36.2)	113.9	(97.0)	—
H_3Ge	Bu^t	**25**	SCF/DZP	81.1	79.3	124.6	108.3	1887i
			MP2/DZP	24.8	(23.0)	106.9	(90.6)	—
			QCISD/DZP[d]	31.8	(30.0)	102.5	(86.2)	—
MeH_2Ge	H	**26**	SCF/DZP	52.6	49.2	113.8	107.7	1955i
			MP2/DZP	35.3	(31.9)	112.4	(106.3)	—
			QCISD/DZP[d]	27.5	(24.4)	115.0	(108.9)	—
MeH_2Ge	Me	**27**	SCF/DZP	81.4	84.1	148.2	133.1	1954i
			MP2/DZP	41.7	(44.4)	143.4	(128.3)	1292i
			QCISD/DZP[d]	42.9	(45.6)	137.0	(122.9)	—
MeH_2Ge	Et	**28**	SCF/DZP	84.0	84.8	140.7	123.9	1965i
			MP2/DZP	38.5	(39.3)	130.7	(113.9)	—
			QCISD/DZP[d]	41.5	(42.3)	125.0	(108.2)	—
MeH_2Ge	Pr^i	**29**	SCF/DZP	85.6	84.8	133.6	116.1	1961i
			MP2/DZP	33.2	(32.4)	118.0	(100.5)	—
			QCISD/DZP[d]	38.4	(37.6)	113.2	(95.7)	—
MeH_2Ge	Bu^t	**30**	SCF/DZP	86.2	83.7	126.3	108.4	1947i
			MP2/DZP	26.5	(24.0)	106.0	(88.1)	—
Me_2HGe	H	**31**	SCF/DZP	52.8	49.4	110.5	103.7	1928i
			MP2/DZP	34.2	(30.8)	108.4	(101.6)	—
			QCISD/DZP[d]	26.6	(23.2)	111.2	(104.4)	—
Me_2HGe	Me	**32**	SCF/DZP	84.2	86.7	147.5	131.4	1976i
			MP2/DZP	42.2	(44.7)	141.0	(124.9)	—
Me_2HGe	Et	**33**	SCF/DZP	87.5	88.1	140.8	123.1	1998i
			MP2/DZP	39.0	(39.6)	128.2	(110.5)	—
Me_2HGe	Pr^i	**34**	SCF/DZP	89.6	88.4	134.1	115.5	1999i
			MP2/DZP	34.7	(33.5)	116.6	(98.0)	—
Me_3Ge	H	**35**	SCF/DZP	53.0	49.9	107.5	100.4	1898i
			MP2/DZP	33.0	(29.9)	104.5	(97.4)	—
			QCISD/DZP[d]	25.6	(22.5)	107.3	(100.2)	—
Me_3Ge	Me	**36**	SCF/DZP	86.8	89.3	147.0	130.4	1992i
			MP2/DZP	42.2	(44.7)	138.3	(121.7)	—
			QCISD/DZP[d]	44.1	(46.6)	132.5	(115.9)	—
Me_3Ge	Et	**37**	SCF/DZP	90.8	91.4	140.9	122.6	2022i
			MP2/DZP	39.5	(40.1)	125.9	(107.6)	—

[a] Energies in kJ mol^{-1}. [b] Frequencies in cm^{-1}. [c] Values in parentheses are estimates based on SCF/DZP ZPE corrections. Values in square brackets are estimates based on MP2/DZP ZPE corrections. [d] QCISD/DZP//MP2/DZP.

radicals respectively with $MeGeH_3$. SCF/DZP + ZPVE calculations suggest barriers of 84.4 ± 0.7 kJ mol^{-1}.

These calculated data are to be compared with available experimental data. Lusztyk and co-workers reported activation energies of 19.7 and 23.1 kJ mol^{-1} for hydrogen abstractions by primary and secondary radicals respectively from tributylgermane.[3] Inclusion of electron correlation serves to lower the calculated forward barriers ($\Delta E_1^{\ddagger}$) for reactions of alkyl radicals to 40.8–42.2 (methyl), 36.9–39.5 (ethyl), 31.8–34.7 (isopropyl) and 24.8–26.5 (*tert*-butyl) kJ mol^{-1} using MP2/DZP. Further single point QCISD/DZP calculations lead to values of 41.7–44.1 (methyl), 40.9–41.5 (ethyl), 36.5–38.4 (isopropyl) and 31.8 kJ mol^{-1} for the single QCISD/DZP calculation performed on a reaction involving the *tert*-butyl radical. Clearly then, for a given alkyl radical, calculated energy barriers ($\Delta E_1^{\ddagger}$) are all within approximately 3 kJ mol^{-1} of each other regardless of the

germane in question and are approximately 20 kJ mol^{-1} higher than the experimentally determined values at the highest level of theory. Similar discrepancies have been reported for analogous calculations involving silicon and tin; possible reasons for these discrepancies have been discussed previously.[14]

It is interesting to note that previous correlated (MP2, QCISD) calculations predict correctly the relative ordering of activation energy ($\Delta E_1^{\ddagger}$) for reactions of alkyl radicals with stannanes and silanes, namely: methyl > primary > secondary > tertiary. In the case of reactions involving germanium, as expected, the same trend is predicted at both MP2/DZP and QCISD/DZP levels of theory. The limited experimental data available (*vide supra*) suggest, at least for primary and secondary radicals, the reverse ordering of $\Delta E_1^{\ddagger}$ (*i.e.* primary < secondary). These experimental results are unusual in that they defy not only the trends predicted by the current calculations, but also the trends observed for the other group(IV) containing hydrides investigated to date. We suggest that perhaps these experimental data should be treated with some degree of caution.

Conclusions

SCF/DZP and MP2/DZP calculations predict that hydrogen atom abstraction reactions by hydrogen atom, methyl, ethyl, isopropyl and *tert*-butyl radicals from several silanes and germanes involve transition states in which the attacking and leaving radicals adopt colinear (or nearly so) arrangements. Activation energies for abstraction of hydrogen atom from several silanes ($\Delta E_1^{\ddagger}$) and germanes are predicted to lie between 25 and 57 kJ mol^{-1} (QCISD) and are some 9–20 kJ mol^{-1} higher than experimentally determined activation energies for analogous reactions with triethylsilane, tributylgermane and TTMSS. These discrepancies may be attributed to solvent, alkyl substitution at silicon, or tunelling effects.[14]

The results presented above indicate that MP2/DZP and QCISD/DZP//MP2/DZP (*ab initio*) calculations are generally capable of reproducing the experimentally observed trends in $\Delta E_1^{\ddagger}$ of primary, secondary and tertiary radicals (*viz.* Et > Pr^{i} > Bu^{t}) toward hydrogen atom abstraction from silanes and germanes.

Interestingly, SCF/DZP, AM1 and AM1 (CI = 2) methods, while predicting similar transition state geometries for reactions involving silanes to the higher-level *ab initio* methods, perform poorly in predicting energy barriers and relative radical reactivities. We urge caution in the use of these methods in modelling silane and germane reductions.

Acknowledgements

We thank the Australian Research Council for financial support and the award of an Australian Postgraduate Award to D. J. H. We also gratefully acknowledge the support of the Ormond Supercomputer Facility, a joint venture of the University of Melbourne and Royal Melbourne Institute of Technology.

References

1 B. Giese, *Radicals in Organic Synthesis: Formation of Carbon–Carbon Bonds*, Pergamon Press, Oxford, 1986.
2 C. Chatgilialoglu, *Acc. Chem. Res.*, 1992, **25**, 188 and references cited therein.
3 J. Lusztyk, B. Maillard, D. A. Lindsay and K. U. Ingold, *J. Am. Chem. Soc.*, 1983, **105**, 3578; L. J. Johnston, J. Lusztyk, D. D. M. Wayner, A. N. Abeywickrema, A. L. J. Beckwith, J. C. Scaiano and K. U. Ingold, *J. Am. Chem. Soc.*, 1985, **107**, 4594; J. Lusztyk, B. Maillard, S. Deycard, D. A. Lindsay and K. U. Ingold, *J. Org. Chem.*, 1987, **52**, 3509.
4 A. G. Davies, *Organotin Chemistry*, VCH, Weinheim, 1997; W. P. Neumann, *Synthesis*, 1987, 665; D. P. Curran, *Synthesis*, 1988, 417; D. P. Curran, *Synthesis*, 1988, 489; C. P. Jasperse, D. P. Curran and T. L. Fevig, *Chem. Rev.*, 1991, **91**, 1237.
5 D. Crich and S. Sun, *J. Org. Chem.*, 1996, **61**, 7200.
6 C. Chatgilialoglu, D. Griller and M. Lesage, *J. Org. Chem.*, 1988, **53**, 3641; M. Ballestri, C. Chatgilialoglu, K. B. Clark, D. Griller, B. Giese and B. Kopping, *J. Org. Chem.*, 1991, **56**, 678.
7 A. L. J. Beckwith and P. E. Pigou, *Aust. J. Chem.*, 1986, **39**, 1151.
8 *The Chemistry of Organic Silicon Compounds*, ed. S. Patai and Z. Rappoport, Wiley, New York, 1989.
9 C. Chatgilialoglu, *Chem. Rev.*, 1995, **95**, 1229 and references cited therein.
10 C. Chatgilialoglu, K. U. Ingold and J. C. Scaiano, *J. Am. Chem. Soc.*, 1981, **103**, 7739; *Landolt-Börnstein*, *Numerical Data and Functional Relationships in Science and Technology*, II/18, ed. H. Fischer, Springer-Verlag, Berlin, 1994.
11 C. H. Schiesser, B. A. Smart and T.-A. Tran, *Tetrahedron*, 1995, **51**, 3327; C. H. Schiesser and B. A. Smart, *Tetrahedron*, 1995, **51**, 6051; see correction in: C. H. Schiesser, B. A. Smart and T.-A. Tran, *Tetrahedron*, 1995, **51**, 10 651; for performance of DZP basis set see: B. A. Smart and C. H. Schiesser, *J. Comput. Chem.*, 1995, **16**, 1055.
12 C. H. Schiesser, M. L. Styles and L. M. Wild, *J. Chem. Soc.*, *Perkin Trans. 2*, 1996, 2257.
13 C. H. Schiesser and M. L. Styles, *J. Chem. Soc.*, *Perkin Trans. 2*, 1997, 2335.
14 D. Dakternieks, D. J. Henry and C. H. Schiesser, *J. Chem. Soc.*, *Perkin Trans. 2*, 1997, 1665.
15 A. Tachibana, Y. Kurosaki, K. Yamaguchi and T. Yamabe, *J. Phys. Chem.*, 1991, **95**, 6849; A. Tachibana, K. Yamaguchi, S. Kawauchi, Y. Kurosaki and T. Yamabe, *J. Am. Chem. Soc.*, 1992, **114**, 7504.
16 M. Guerra, *J. Am. Chem. Soc.*, 1993, **115**, 11 926.
17 Y.-D. Wu and C.-L. Wong, *J. Org. Chem.*, 1995, **60**, 821.
18 M. S. Gordon, D. R. Gano and J. R. Boatz, *J. Am. Chem. Soc.*, 1983, **105**, 5771; M. B. Coolidge, D. A. Hrovat and W. T. Border, *J. Am. Chem. Soc.*, 1992, **114**, 2354.
19 L. Ding and P. Marshall, *J. Am. Chem. Soc.*, 1992, **114**, 5754.
20 M. J. Frisch, G. W. Trucks, M. Head-Gordon, P. M. W. Gill, M. W. Wong, J. B. Foresman, B. G. Johnson, H. B. Schlegel, M. A. Robb, E. S. Replogle, R. Gomperts, J. L. Andres, K. Raghavachari, J. S. Binkley, C. Gonzales, R. L. Martin, D. J. Fox, D. J. Defrees, J. Baker, J. J. P. Stewart and J. A. Pople, GAUSSIAN92, Revision F, Gaussian Inc., Pittsburgh, PA, 1992.
21 M. J. Frisch, G. W. Trucks, H. B. Schlegel, P. M. W. Gill, B. G. Johnson, M. A. Robb, J. R. Cheeseman, T. Keith, G. A. Petersson, J. A. Montgomery, K. Raghavachari, M. A. Al-Laham, V. G. Zakrzewski, J. V. Ortiz, J. B. Foresman, C. Y. Peng, P. Y. Ayala, W. Chen, M. W. Wong, J. L. Andres, E. S. Replogle, R. Gomperts, R. L. Martin, D. J. Fox, J. S. Binkley, D. J. Defrees, J. Baker, J. J. P. Stewart, M. Head-Gordon, C. Gonzalez and J. A. Pople, GAUSSIAN94, Revision B.3, Gaussian Inc., Pittsburgh, PA, 1995.
22 W. J. Hehre, L. Radom, P. v. R. Schleyer and P. A. Pople, *Ab Initio Molecular Orbital Theory*, Wiley, New York, 1986.
23 AMPAC 5.0, © 1994 Semichem, 7128 Summitt, Shawnee, KS 66 216.
24 W. Adcock, C. I. Clark and C. H. Schiesser, *J. Am. Chem. Soc.*, 1996, **118** 11 541.
25 C. H. Schiesser and M. A. Skidmore, *J. Organomet. Chem.*, in the press.

Paper 7/07692D
Received 24*th October* 1997
Accepted 22*nd December* 1997